2019 IEEE World Haptics Conference (WHC)
Tokyo, Japan
9-12 July 2019

Artificial Fingers Wearing Skin Vibration Sensor for Evaluating Tactile Sensations*

Yoshihiro Tanaka[1], Tatsuya Hasegawa[1], Masatoshi Hashimoto[2], and Takanori Igarashi[2]

***Abstract*— Tactile sensations are based on stimulation elicited on the skin through mechanical interaction between the skin and an object. It is important to consider skin properties in addition to the object. We developed a wearable skin vibration sensor and previously showed the availability for texture evaluations. However, the sensor output is not reproducible because human skin cannot maintain the same condition. Thus, we propose using artificial fingers. The artificial finger is worn on a human finger and the skin vibration sensor is wrapped on the artificial finger in the same way as the sensor would be mounted on a human finger. The artificial finger consists of a rigid base, a soft layer, and a thin layer having ridge on the surface, and can be easily exchanged to other finger with different properties. Experiments with different artificial fingers for particle surfaces show that the sensor output has a relation with particle size, and the height of the ridge influences the intensity of the sensor output and the groove width influences the peak frequency and the measuring range. Results indicate that the proposed artificial finger might be useful for tactile evaluations, reflecting different skin properties and customizing towards target objects and users.**

I. INTRODUCTION

The evaluation of tactile sensations is desired for the development and quality assurance of products, development of tactile devices, and tactile perception research. Many basic studies on tactile perception have examined physical information from objects, e.g., spatial information, stiffness, and others [1][2]. The findings from these studies provide useful knowledge for evaluating tactile sensations and designing tactile devices. However, tactile sensations are based on pressure, vibration, and temperature changes elicited on the skin through mechanical interaction between the skin and an object. Analysis and evaluation based on mechanical stimulation elicited on the skin directly represents tactile sensations. Indeed, skin has specific characteristics, and object information can be coded on the skin. Some previous works showed that epidermal ridges enhance vibration when an object is rubbed with the finger pad [3][4]. Tanaka et al. [5] and Matsuura et al. [6] showed that the vibration transfer function elicited on the human finger pad has a peak frequency ranging from 100 to 300 Hz. FEM analysis with a skin model shows that the epidermal ridge, dermal ridge, multiple layers with different stiffnesses of fingers, or collagen fibers affect deformation of the finger pad and stress distribution inside the finger pad [7][8][9]. It is important to consider the properties of the skin, contact object, and exploratory movements.

Recently, the relationship between mechanical stimulation on the skin and contact object, and that between mechanical stimulation and tactile sensations like roughness, have been investigated. Delhaye et al. [10], Manfredi et. al [11], and Natsume et al. [12] measured skin vibration while textures were rubbed with a bare fingertip and determined the relationship between skin vibration and spatial information on the surfaces. Bensmia et al. [13] showed that skin vibration weighted by the sensitivity of Pacinian corpuscles, which are mechanoreceptors, sufficiently accounts for textural discrimination based on roughness. Natsume et al. [14] showed that skin vibration better represents the roughness ratings of participants compared with classical roughness parameters like Ra (arithmetic mean roughness). Furthermore, it was recently demonstrated that the neural code based on mechanoreceptors accounts for roughness ratings and roughness discrimination [15][16].

There are individual differences in the properties of human skin, thus mechanical stimulation on the skin is inherently different among individuals. The thickness and stiffness of the skin varies based on gender and age [17]. Peters et al. showed that discrimination sensitivity of spatial information tended to be higher in females than in males [18]. They determined the relationship between sensitivity and contact area, and they claimed that the finger size determines tactile acuity. Thus, mechanical stimulation elicited on the skin is useful for representing tactile sensations, and the consideration of individual differences in skin properties may allow individual tactile sensations to be evaluated.

Tanaka et al. developed a wearable tactile sensor that detects skin-propagated vibration [19]. The sensor is made of a polymer piezo material, where the sensor is wrapped on the middle phalanx of the index finger. This allows users to touch objects with a bare finger pad. Therefore, the sensor output is determined by skin and object properties. Previous experiments showed that the collected data sufficiently reflected the roughness ratings provided by each participant [12][14]. However, it is difficult to obtain reproducible and stable data because human skin cannot inherently maintain the same condition. Thus, we have proposed using artificial fingers instead of a human finger [20]. The proposed sensor is shown in Fig. 1. The artificial finger can be worn on the finger and the wearable skin vibration sensor is mounted on the artificial finger in the same way as the sensor would be mounted on a

*This work was supported by Kao corporation

[1]Yoshihiro Tanaka and Tatsuya Hasegawa are with Department of Electrical and Mechanical Engineering, Graduate school of Engineering, Nagoya Institute of Technology, Gokiso-cho, Showa-ku, Nagoya 466-8555, Japan tanaka.yoshihiro@nitech.ac.jp

[2]Masatoshi Hashimoto and Takanori Igarashi are with Skincare Products Research, Kao Corporation, 2-1-3 Bunka, Sumida-ku, Tokyo 131-8501, Japan hashimoto.masatoshi@kao.com, igarashi.takanori@kao.com

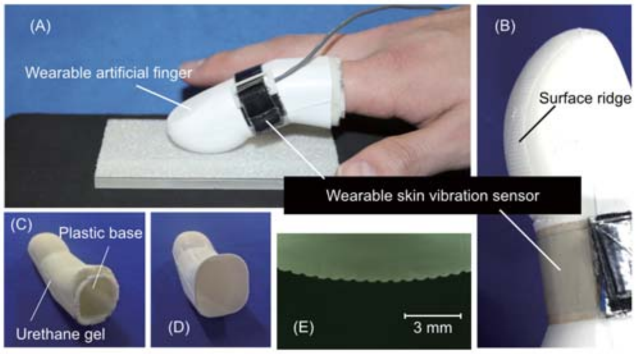

Fig. 1. Artificial finger wearing a skin vibration sensor. (A) and (B) Overview of the artificial finger worn to a human finger. The skin vibration sensor is wrapped on the artificial finger. (C) Plastic base part of a rigid body like a bone and urethane gel covering the base in order to mimic the subcutaneous tissue and dermis (D) Silicone rubber covering the urethane gel. It is used as epidermis of the human finger, and the silicone rubber has horizontal striped ridges on the area corresponding to the finger pad that mimic epidermal ridges. (E) Example of ridges on silicone rubber surface.

human finger. The artificial finger has a rigid base; thus, the sensor output is not influenced by the properties of the human finger. Many artificial fingers with tactile sensors have been proposed in other studies [21][22][23][24][25]. However, they have been mounted on robot arms and operation system like a slider and sensing elements were embedded in fingers or system. It seems that exchanging the finger is not easy. In our proposed sensor, an artificial finger can be easily exchanged because the wearable skin vibration sensor is wrapped on the finger. Moreover, this method allows the sensor output from the artificial finger to be compared with the sensor output from the human finger. Thus, the proposed sensor with an artificial finger might be useful for reflecting individual characteristics of each person's finger, evaluating tactile information, and customizing towards target objects and users. In addition, results with different artificial fingers might provide useful knowledge for basic tactile research. There are many wearable tactile sensors like artificial skin [26][27][28], but many studies aimed to measure forces or deformations applied to fingers as interfaces and have not focused on different fingers towards tactile evaluations.

In this study, we investigate the applicability of a wearable artificial finger with a wearable skin vibration sensor for evaluating tactile information. Previous studies with human fingers showed that the wearable skin vibration sensor is useful for evaluating perceived roughness [12][14]. Thus, glass particle surfaces with different diameters are used for the current paper. Sensor output for different roughness and effect of different artificial fingers are investigated. Artificial fingers can change mechanical properties in dimensions, stiffness, and thickness of each layer, and surface ridges. The epidermal ridge is one important factor that influences skin vibration [3][4][7][29][30]. The effect of ridge height was investigated in a previous study [20]. This paper investigates the influence of the height and groove width of the ridge on the artificial finger surface. The results show the usefulness of the proposed artificial finger and different evaluation characteristics of different artificial fingers.

II. ARTIFICIAL FINGER WEARING SKIN VIBRATION SENSOR

A. Basic Idea

Herein, we propose expanding a wearable skin vibration sensor [19] to use in wearable artificial fingers. Reproducible and stable data can be collected with artificial fingers compared with human fingers. The wearable skin vibration sensor is wrapped on an artificial finger in the same way as it would be on a human finger. Thus, the findings obtained with human fingers are available to the analysis and evaluation with artificial fingers. Furthermore, this method allows artificial fingers to be easily exchanged. This indicates that skin properties of the artificial finger like stiffness, surface ridges, and others can be easily adapted to use with target objects and/or persons. It might be possible to change the skin properties in order to enhance object discrimination or reflect each person's skin. In addition to evaluation, results with different artificial fingers might provide useful knowledge on tactile perception research.

Furthermore, a wearable finger can utilize human exploratory movements. Humans use contact force and scanning velocity in exploratory movements for tactile perception. Usually, human exploratory movement are difficult to reproduce with robot arms and fingers because they often require multi-DOF arms and fingers, as well as complex strategies. Even if such human movements can be mimicked with robots, such robots tend to require complex and huge system, and vibration induced by movements of robot arms and fingers during the exploration creates a noise problem. In the future, the proposed wearable artificial finger with the sensor could bridge the evaluation by humans to that by robots. Findings with the wearable artificial finger might provide useful knowledge for evaluating tactile information with robots.

From these aspects, in particular, the base of an artificial finger was designed to be a rigid body in order to prevent the human finger from affecting the sensor output. In the future, other sensors (e.g., pressure and temperature) could be embedded to expand the sensor for evaluating a broader range of tactile information.

B. Structure

The wearable artificial finger consists of a plastic base, urethane gel (HITOHADA gel, EXSEAL), and silicone rubber (KE-14, ShinEtsu). The bottom of Fig. 1 shows the base with urethane gel, silicone rubber, and the surface on silicone rubber. The base is hard and can function as a rigid body, like a bone. The urethane gel (thickness: about 2.5 mm, Young's modulus: 0.06 MPa) covers the base in order to mimic the subcutaneous tissue and dermis of a human finger [7]. Silicone rubber (thickness: about 1 mm. Young's modulus: 0.70 MPa) covers the urethane gel and is harder than the urethane gel. It is used as epidermis of the human finger, and the silicone rubber has horizontal striped ridges perpendicular to the longitudinal direction of the fingers on the area corresponding to the finger pad that mimic epidermal

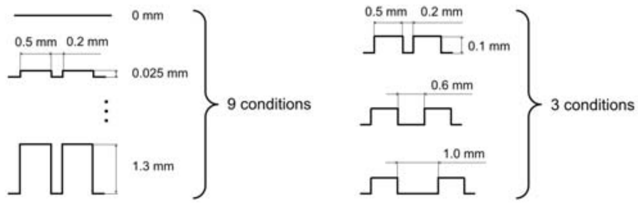

Fig. 2. Experimental conditions of surface ridge of artificial fingers.

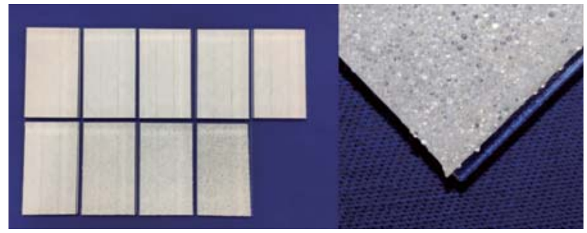

Fig. 3. Sample stimuli.

TABLE I

AVERAGE PARTICLE SIZE AND THE RANGE.

No	Average particle size [μm]	No	Average particle size [μm]
1	50 (37–63)	6	425 (350–500)
2	76 (63–88)	7	605 (500–710)
3	115 (105–125)	8	850 (710–990)
4	163 (149–177)	9	1194 (991–1397)
5	214 (177–250)		

ridges. We can change the hardness of the urethane gel and silicone rubber, and ridges can be designed on the silicone rubber.

III. EXPERIMENTAL METHODS

A. Conditions

We prepared different ridges on the surface of the silicone rubber to investigate the effect of roughness on the sensor output. Fig. 2 indicates these conditions. Two kinds of experiments were conducted. The first experiment examined the influence of ridge height and the second examined the influence of the groove width in a ridge on the sensor output.

As shown in the left panel of Fig. 2, we prepared ridges with 9 different heights (0 (no ridge), 0.025, 0.05, 0.075, 0.1, 0.4, 0.7, 1.0, and 1.3 mm) for the first experiment. The groove and ridge width were 0.2 and 0.5 mm, respectively. As shown in the right panel of Fig. 2, we prepared 3 different groove widths (0.2, 0.6, and 1.0 mm) for the second experiment. The ridge width and height were determined to be 0.5 and 0.1 mm, respectively.

These parameters were determined in the consideration of the dimensions of human epidermal ridges [7][31]. Maeno et al. [31] measured the dimensions of the epidermal ridge for twenty human fingers defining it as arc or trapezoid, and showed that mean height was about 0.1 mm and the width involving the grooved and ridge part was about 0.5 mm. Therefore, the artificial finger with ridges of 0.1 mm height, 0.5 mm width, and 0.2 mm groove width was the closest to human finger of all artificial fingers prepared.

B. Sample Stimuli

Nine sample stimuli with different roughness values were used for the experiments as shown in Fig. 3. We used the same samples as those used in previous studies [12]. These surfaces contained glass particles. Glass particles with a given diameter were attached on the surface of a flat acrylic plate with double-sided tape [32]. The glass particles did not have sharp edges and its size distribution was certified by the distributor (KENIS Ltd.). Table 1 shows the average particle size and its range on each surface.

C. Experimental Setup

Each sample was placed on a stage and a 6-axis force sensor (Gamma, ATI) was placed on the bottom of the stage to measure the exerted normal force. The wearable artificial finger with the skin vibration sensor was placed on the index finger of an experimenter. The experimenter rubbed each surface with a contact force of approximately 0.3 N and scanning velocity of approximately 150 mm/s from backward to forward as shown in Fig. 1 (A). These behavior conditions were determined within natural active roughness perception of humans [33]. The experimenter could maintain the contact force near 0.3 N by watching a live profile of the contact force on a monitor, and the scanning velocity was maintained near 150 mm/s by listening a metronome. 5 rubbing strokes were used for each surface.

The sensor output and normal force were collected with a DAQ module (NI-USB-6218, National Instruments) with 10 kHz sampling frequency. A high-pass filter with 10 Hz cutoff frequency was applied into the output from the skin vibration sensor and a low-pass filter with 10 Hz cutoff frequency was applied into the output from the force sensor.

D. Signal Processing

The sensor output was extracted from the data collected during each stroke. In the same way as in previous research [14], the stable period for one stroke was found to be 0.3 s (i.e., 0.15 s before and after the midpoint). The period was defined using the exerted normal force; the central point was calculated using the time interval where the exerted normal force was greater than 0.075 N.

The power spectral density was calculated from the extracted data and the sum of the power spectral density was calculated as an evaluation parameter that indicates the intensity of the vibration as follows:

$$V_{PSD} = \log_{10} \int_{10}^{1000} PSD_{rub}(f) df \qquad (1),$$

where f [Hz] is frequency and PSD_{rub} is the power spectral density. The mean vibration intensity was calculated from 5 strokes on each surface.

IV. RESULTS

A. Experiment I: Height

Typical power spectral density for each ridge height is shown in Fig. 4. Mean power spectral density for each frequency calculated from 5 strokes with sample No. 6 (425 μm diameter) is presented for each artificial finger. In general, the power spectral densities decreased at high frequency with all artificial fingers, similar to the case with

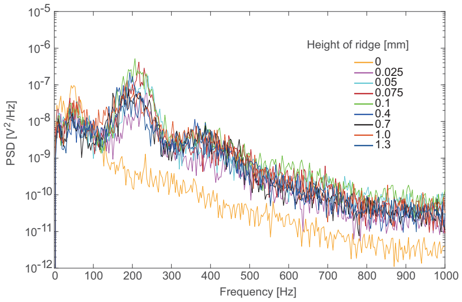

Fig. 4. Power spectral densities with sample No. 6 on artificial fingers with different ridge heights.

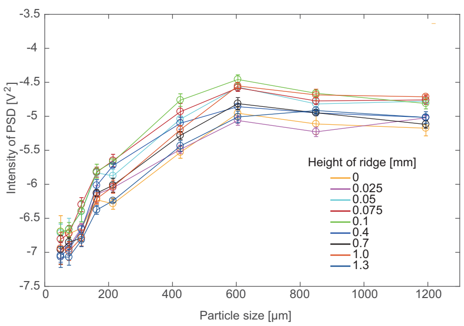

Fig. 5. Intensity of sensor output on all samples for each artificial finger with different ridge height.

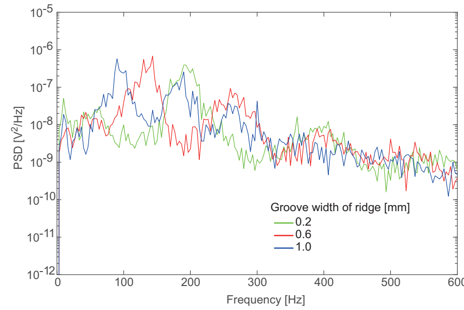

Fig. 6. Power spectral densities with sample No. 6 on artificial fingers with different groove widths.

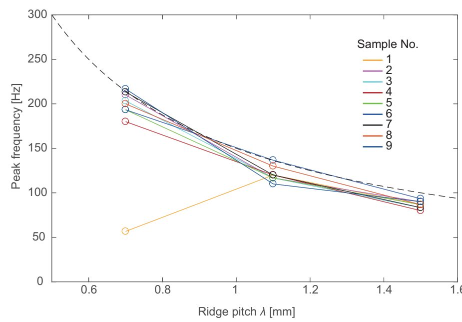

Fig. 7. Peak frequency on each surface for artificial fingers with different groove widths. A dashed line indicates the estimates by Eq. (3).

human fingers [14]. Comparing the power spectral densities among artificial fingers, the sensor outputs from artificial fingers with ridges exhibit a distinct peak frequency near 200 Hz where the power spectral density reached a large value. However, the sensor output from the artificial finger without ridges did not appear to have a peak frequency.

Fig. 5 shows the intensity of the sensor output with each particle size for each artificial finger. Each plot indicates the mean intensity and its standard deviation calculated using data from 5 strokes. One can see that the intensity increased as the particle size increased while remaining less than approximately 600 μm. The result shows that artificial fingers without/with different ridges produced sensor outputs with different intensities. The output intensity from the artificial finger with 0, 0.025, and 1.3 mm ridges was relatively small, while that from the artificial finger with 0.1 mm ridges was relatively large.

B. Experiment II: Groove Width

Typical power spectral density for each groove width of the ridge is shown in Fig. 6. Mean power spectral density for each frequency calculated from 5 strokes with sample No. 6 (425 μm diameter) is presented for each artificial finger. In contrast to the results with different ridge heights, the sensor output for artificial fingers with different widths had different peak frequencies in the power spectral density.

Then, we calculated peak frequency with each sample for each artificial finger as follows:

$$f_p = \underset{30 \le f}{\arg\max}\, PSD_{rub}(f) \quad (2).$$

In addition to the obtained peak frequency, we estimated the peak frequency. Considering the pitch λ involving the groove and ridge width and the scanning velocity v, the peak frequency is estimated as

$$\hat{f}_p = \frac{v}{\lambda} \quad (3).$$

Fig. 7 shows the peak frequencies obtained from the experimental results and the value estimated with Eq. (3). The estimated value is indicated with a dashed line.

In addition to the peak frequency, we also calculated intensity of the sensor output for each sample. Fig. 8 shows the mean intensity and its standard deviation for artificial fingers with different widths on each surface. The results show that the intensities among the artificial fingers are similar for particle sizes less than 600 μm. However, the intensity differed among artificial fingers on particle sizes larger than 800 μm. In particular, the sensor output from the artificial finger with 0.2 mm groove width decreased when the particle size was larger than 800 μm. The sensor output for artificial fingers with 0.6 and 1.0 mm groove width increased as the particle size increased among all prepared particles, whereas the variance in the sensor output was relatively small with large particle sizes compared with small particle sizes.

V. DISCUSSION

Experimental results show that the sensor output increased overall as the particle size increased, especially regarding smaller particles. This result is similar to results from previous studies involving measurement of skin vibration with the wearable sensor [12]. Thus, the results indicate that our proposed sensor with an artificial finger is useful for gathering tactile information.

Then, we will discuss the influence of different artificial fingers. First, let us discuss the influence of ridge height on

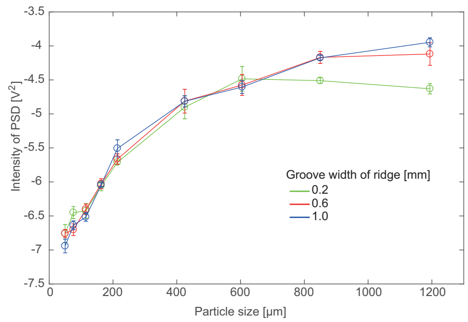

Fig. 8. Intensity of sensor output on all samples for each artificial finger with different groove width.

the artificial finger's surface in consideration of the human epidermal ridge. The experimental results showed that the presence of the ridge induced large sensor output for a specific frequency. An artificial finger without ridges on the surface did not have a peak frequency. Scheibert et al. [3] showed that the epidermal ridge weighs the vibration elicited by rubbing textures at a specific frequency according to the ridge pitch and the scanning velocity. All artificial fingers with ridges of different heights and the same pitch appeared to exhibit a similar peak frequency. This result is consistent with the previous findings. Regarding the intensity of the sensor output, artificial fingers with ridge height of 0, 0.025, and 1.3 mm had relatively small intensity, and the artificial finger with 0.1 mm ridges tended to output relatively large intensity. This might be caused by ridges with different lengths and stiffnesses. The peak frequency indicates the effect of the ridges. Higher ridges induce large vibration via a lever mechanism, but the stiffness of the ridge is also relevant for eliciting a large vibration. Assuming the ridge operates like a cantilevered beam, the relationship between the load P and deflection at the edge of the ridge δ is

$$P = \frac{3EI}{l^3}\delta \qquad (4),$$

where E is Young's modulus, I is the moment of inertia, and l is the length of the ridge (height). Therefore, the height largely influences the stiffness of the ridge, and a longer ridge makes the ridge softer. Stiffness adequate to the soft base of the artificial finger, which is composed of silicone rubber and urethane gel, might elicit large surface vibrations.

Next, let us discuss the influence of the groove width on the surface of the artificial finger. The result showed that each artificial finger had different peak frequency in the power spectral density. Fig. 7 shows that the obtained peak frequencies were similar to those estimated using the scanning velocity and pitch (Eq. (3)). The result is consistent with previous findings that showed the effect of the human epidermal ridge [3][4][29][30]. Here, each surface contained particles with different diameters, as shown in Table 1, but the particles were not periodically distributed on the surface with a particular same pitch [12][32]. Thus, the pitch on the surface might not dominantly affect the peak frequency. Previous works with periodic surfaces and stimulation showed the influence of the object surface pitch in addition to the scanning velocity, having the interaction with the epidermal ridge [29][30][34]. We will investigate the response to periodic surfaces. The peak frequency on sample No. 1 (50 μm diameter) for the artificial finger with 0.2 mm groove width was remarkably less than the estimated value. This might be caused by a low intensity sensor output.

Regarding the intensity of the sensor output, the result shows that the sensor outputs from artificial fingers with different groove widths were similar on a given surface with particle size less than 600 μm. In the second experiment, the height and width of the ridge were the same, and only groove width was different. Therefore, the stiffness of the ridge might be similar among artificial fingers. This result is consistent with the discussion regarding results from the first experiment. However, the intensity of the sensor output due to rubbing on particles larger than 800 μm was different among artificial fingers. In particular, the sensor output from the artificial finger with 0.2 mm groove width decreased on surfaces with particle size larger than 800 μm. We can observe similar tendencies in the first experiment with the same groove width. This might be caused by the relative dimensions between the particle size and the groove width. Fig. 9 shows the mechanical interaction between the ridge and particles. Each panel shows the case with 0.2 mm groove width and 1.0 mm groove width on a 1200 μm particle surface. The pitch among each particle is distributed near 1200 μm, depending on the diameter of the particle. Therefore, when the grooved width is much smaller than the diameter of the particle, as in the case of the 0.2 mm groove width, the effect of the ridge as mentioned in the first experiment might not be strongly expected because the ridge could hardly penetrate the gap between particles on the object surface. Thus, the sensor output from the artificial finger with 0.2 mm groove width decreased with large particles.

As a general discussion, the results showed that the ridge of the artificial finger enhances the sensor output (skin vibration), as occurs with ridges on the human epidermis. The height of the ridge influenced the intensity of the sensor output, and the groove width influenced the peak frequency and the measuring range. The results show that different artificial fingers reflect different mechanical interactions when rubbing the surface of an object. This indicates that the artificial finger is useful for evaluating tactile information and could be used to evaluate individual tactile information reflecting the skin characteristics of each person and/or enhance the sensor output according to target objects.

In the current study, we have focused on the ridge on the artificial finger, but the softness of the artificial finger also influences the sensor output. Previous related works with artificial fingers showed that multiple layers of the finger pad and viscoelastic properties influence the friction characteristic [24][25]. In the future, we will investigate the influence of the silicone rubber and the urethane gel of the artificial finger. And human fingertip ridges are not exactly horizontal as our artificial fingers [4]. Since the pattern of ridges may affect vibrations elicited, we will investigate it. In addition, we will investigate a method for designing the artificial finger and calibrating the sensor output in order to

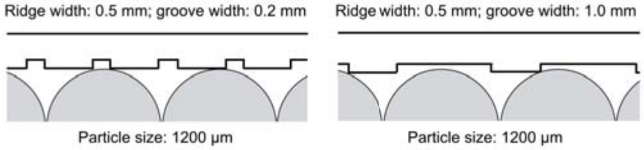

Fig. 9. Images of mechanical interaction between ridges of the artificial finger and particles.

reflect individual human finger characteristics on the artificial finger. Moreover, multi-force and temperature sensors could be embedded on the base part of the artificial finger and be used to evaluate a broader range of tactile information.

VI. CONCLUSIONS

This paper presented a wearable artificial finger with a skin vibration sensor. The skin vibration sensor is wrapped on the artificial finger in the same way as the sensor would be mounted on a human finger. The artificial finger consists of a rigid base, a soft layer, and a thin layer having ridge on the surface in the consideration of human skin. Artificial fingers with different skin properties can be easily exchanged. In the present paper, artificial fingers with different ridges were prepared and the sensor output when rubbing different particle surfaces were collected. The sensor output overall increased with the rise of particle size in particular on the small size. Furthermore, the sensor output had different tendencies depending on different artificial fingers. The height of the ridge influenced the intensity of the sensor output and the groove width influenced the peak frequency and the measuring range. The results showed that the proposed artificial finger is available for the evaluation of tactile information and different artificial fingers have different response reflecting skin properties. This indicates that the artificial finger might be useful for customizing towards target objects and users in order to evaluate the object more precisely and reflect individual characteristics of each person's finger.

REFERENCES

[1] S. J. Lederman, M. M. Taylor, Fingertip force, surface geometry, and the perception of roughness by active touch, Percept. Psychophys., vol. 12, pp. 401–408, 1972.

[2] W. M. Bergmann Tiest, A. M. L. Kappers, Haptic and visual perception of roughness, Acta. Psychol. (Amst), vol. 124, pp. 177–189, 2007.

[3] J. Scheibert, S. Leurent, A. Prevost, G. Debregeas, The role of fingerprints in the coding of tactile information probed with a biomimetic sensor, Science, vol. 323, pp. 1503–1506, 2009.

[4] A. Prevost, J. Scheibert, G. Debregeas, Effect of fingerprints orientation on skin vibrations during tactile exploration of textured surfaces, Commun Integr Biol, vol. 2, no. 5, pp. 422–424, 2009.

[5] Y. Tanaka, Y. Horita, A. Sano, Finger-mounted skin vibration sensor for active touch, Proc. Eurohaptics 2012, pp. 169-174, 2012.

[6] Y. Matsuura, S. Okamoto, Y. Yamada, Estimation of finger pad deformation based on skin deformation transferred to the radial side, Proc. Eurohaptics 2014, pp. 313–319, 2014.

[7] T. Maeno, K. Kobayashi, N. Yamazaki, Relationship between the structure of human finger tissue and the location of tactile receptors, JSME Int. J. Ser. C, vol. 41, pp. 94–100, 1998.

[8] K. Dandekar, B. I. Raju, M. A. Srinivasan, 3-d finite-element models of human and monkey fingertips to investigate the mechanics of tactile sense, J. Biomech. Eng-Trans. ASME, vol. 118, pp. 48–55, 2003.

[9] Y. Tanaka, T. Ito, M. Hashimoto, M. Fukasawa, N. Usuda, A. Sano, Collagen fibers induce expansion of receptive field of Pacinian corpuscles, Adv. Robot., vol. 29, pp. 735–741, 2015.

[10] B. Delhaye, V. Hayward, P. Lefevre, J. L. Thonnard, Texture-Induced vibrations in the forearm during tactile exploration, Front. Behav. Neurosci., vol. 6, 37, 2012.

[11] L. R. Manfredi, H. P. Saal, K. J. Brown, M. C. Zielinski, J. F. Dammann 3rd, V. S. Polashock, S. J. Bensmaia, Natural scenes in tactile texture, J. Neurophysiol., vol. 111, pp. 1792–1802, 2014.

[12] M. Natsume, Y. Tanaka, A. M. L. Kappers, Individual differences in cognitive processing for roughness rating of fine and coarse textures, PLoS ONE, vol. 14, e0211407, 2019.

[13] S. Bensmaia, M. Hollins, Pacinian representations of fine surface texture, Percept. Psychophys., vol. 67, pp. 842–854, 2005.

[14] M. Natsume, Y. Tanaka, W. M. Bergmann Tiest, A. M. L. Kappers, Skin vibration and contact force in active perception for roughness perception, Proc. 26th IEEE RO-MAN, pp. 1479–1484, 2017.

[15] J. D. Lieber, X. Xia, A. I. Weber, S. J. Bensmaia, The neural code for tactile roughness in the somatosensory nerves, J. Neurophysiol., vol. 118, pp. 3107–3117, 2017.

[16] A. I. Weber, H. P. Saal, J. D. Lieber, J. W. Cheng, L. R. Manfredi, J. F. Dammann 3rd, S. J. Bensmaia, Spatial and temporal codes mediate the tactile perception of natural textures, PNAS, vol. 110, pp. 17107–17112, 2013.

[17] P. D. Agache, C. Monneur, J. L. Leveque, J. De Rigal, Mechanical properties and Young's modulus of human skin in vivo, Arch. Dermatol. Res., Vol. 269, pp. 221-232, 1980.

[18] R. M. Peters, E. Hackeman, D. Goldreich, Diminutive digits discern delicate details: fingertip size and the sex difference in tactile spatial acuity, J. Neurosci., vol. 29, pp. 15756–15761, 2009.

[19] Y. Tanaka, D. P. Nguyen, T. Fukuda, A. Sano, Wearable skin vibration sensor using a PVDF film, Proc. 2015 IEEE World Haptics Conference, pp. 146–151, 2015.

[20] Y. Tanaka, M. Hashimoto, T. Igarashi, Artificial finger for tactile evaluation based on skin vibration, Proc. SICE SI2018 Annual Conference, pp. 1350–1351, 2018 (In Japanese).

[21] S. Chen, S. Ge, W. Tang, J. Zhang, N. Chen, Tactile perception of fabrics with an artificial finger compared to human sensing, Textile Research Journal, vol. 85, pp. 2177–2187, 2015

[22] Y. Mukaibo, H. Shirado, M. Konyo, T. Maeno, Development of a texture sensor emulating the tissue structure and perceptual mechanism of human fingers, Proc. 2005 IEEE ICRA, pp. 2576–2581, 2005.

[23] H. Tsutsui, Y. Murashima, N. Honma, K. Kobayashi, Development of multichannel soft tactile sensors having fingerprint structure, Conf Proc IEEE Eng Med Biol Soc, pp. 2496–2499, 2014.

[24] F. Shao, T. H. C. Childs, B. Henson, Developing an artificial fingertip with human friction properties, Tribol Int, vol. 42, pp. 1575–1581, 2009.

[25] R. F. Friesen, M. Wiertlewski, M. A. Peshkin and J. E. Colgate, Bioinspired artificial fingertips that exhibit friction, Proc. 2015 IEEE World Haptics Conference, pp. 208–213, 2015.

[26] B. Li, Y. Shi, A. K. Fontecchio, Y. Visell, Mechanical imaging of soft tissues with a highly compliant tactile sensing array, IEEE Trans. Biomed. Eng., 65, pp. 687–697, 2018.

[27] F. L. Hammond, Y. Menguc, R. J. Wood, Toward a modular soft sensor-embedded glove for human hand motion and tactile pressure measurement, Proc. IROS 2014, pp. 4000–4007, 2014.

[28] T. Takei, M. Ando, H. Mochiyama, Wearable artificial skin layer for the reconstruction of touched geometry by morphological computation, Adv. Robot., vol. 32, pp. 1–13, 2018.

[29] R. Fagiani, M. Barbieri, Modeling of finger-surface contact dynamics, Tribol Int, vol. 74, pp. 130–137, 2014.

[30] R. Fagiani, F. Massi, E. Chatelet, Y. Berthier, A. Akay, Tactile perception by friction-induced vibrations, Tribol Int, vol. 44, pp. 1100–1110, 2011.

[31] T. Maeno, D. Yamada, H. Sato, Analysis on Geometry of Human Epidermal Ridges, Trans JSME Ser. C, vol. 71, pp. 245–250, 2005 (In Japanese).

[32] H. Tsuboi, M. Inoue, S. Kuroki, H. Mochiyama, J. Watanabe, Roughness perception of micro-particulate plate: A study on two-size-mixed stimuli, Proc. EuroHaptics 2014, pp. 446–452, 2014.

[33] Y. Tanaka, W. M. Bergmann Tiest, A. M. L. Kappers, A. Sano, Contact force and scanning velocity during active roughness perception. PLoS ONE, vol. 9, e93363, 2014 .

[34] Y. Vardar, B. Guclu, and C. Basdogan, Effect of waveform on tactile perception by electrovibration displayed on touch screens, IEEE Trans Haptics, vol. 10, no. 4, pp.488–499, 2017.